Available online at www.sciencedirect.com
ScienceDirect
Journal of Environmental Sciences 2010, 22(9) 1447–1454
JOURNAL OF ENVIRONMENTAL SCIENCES
ISSN 1001-0742
CN 11-2629/X
www.jesc.ac.cn

Iron-doped Mn-Ce/TiO_2 catalyst for low temperature selective catalytic reduction of NO with NH_3

Boxiong Shen*, Ting Liu, Ning Zhao, Xiaoyan Yang, Lidan Deng

College of Environmental Science and Engineering, Nankai University, Tianjin 300071, China.
E-mail: shenboxiong0722@sina.com

Received 25 November 2009; revised 03 February 2010; accepted 09 March 2010

Abstract

The catalysts of iron-doped Mn-Ce/TiO_2 (Fe-Mn-Ce/TiO_2) prepared by sol-gel method were investigated for low temperature selective catalytic reduction (SCR) of NO with NH_3. It was found that the NO conversion over Fe-Mn-Ce/TiO_2 was obviously improved after iron doping compared with that over Mn-Ce/TiO_2. Fe-Mn-Ce/TiO_2 with the molar ratio of Fe/Ti = 0.1 exhibited the highest activity. The results showed that 96.8% NO conversion was obtained over Fe(0.1)-Mn-Ce/TiO_2 at 180°C at a space velocity of 50,000 hr^{-1}. Fe-Mn-Ce/TiO_2 exhibited much higher resistance to H_2O and SO_2 than that of Mn-Ce/TiO_2. The properties of the catalysts were characterized using X-ray diffraction (XRD), N_2 adsorption, temperature programmed desorption (NH_3-TPD and NO*x*-TPD), and X-ray photoelectron spectroscopy (XPS) techniques. BET, NH_3-TPD and NO*x*-TPD results showed that the specific surface area and NH_3 and NO*x* adsorption capacity of the catalysts increased with iron doping. It was known from XPS analysis that iron valence state on the surface of the catalysts were in Fe^{3+} state. The doping of iron enhanced the dispersion and oxidation state of Mn and Ce on the surface of the catalysts. The oxygen concentrations on the surface of the catalysts were found to increase after iron doping. Fe-Mn-Ce/TiO_2 represented a promising catalyst for low temperature SCR of NO with NH_3 in the presence of H_2O and SO_2.

Key words: low-temperature SCR; Fe-Mn-Ce/TiO_2; H_2O; SO_2

DOI: 10.1016/S1001-0742(09)60274-6

Introduction

Low temperature selective catalytic reduction (SCR) of nitrogen oxides (NO*x*) with ammonia (NH_3) is a promising technique to remove NO*x* in flue gases from stationary sources. The low temperature SCR unit can be located downstream of the particulate control device and desulfurizer without heating, which results in systems of low energy consumption and retrofitting easily into the boiler system. However, there is still residual SO_2 remaining after desulfurizer. The deactivation of the low temperature SCR catalysts by SO_2 in the flue gases limits the utilization of these catalysts under practical conditions. So the catalyst deactivation by residue SO_2 should be considering.

Manganese oxides contained various types of labile oxygen which were believed to play an important role in the SCR catalytic circle (Park et al., 2001). Ceria (CeO_2) has been studied extensively due to its property as an oxygen reservoir, which stores and releases oxygen via the redox shift between Ce^{4+} and Ce^{3+} (Xu et al., 2008). Due to its redox properties, CeO_2 could enhance the oxidation of NO to NO_2, which were favorable to the low-temperature SCR of NO with NH_3.

Mn-Ce mixed-oxide catalysts have also been studied as low temperature SCR catalysts. Qi et al. (2004) developed MnO_x-CeO_2 mixed oxides with superior activity for low-temperature SCR of NO with NH_3 in the absence of SO_2, but small concentrations of SO_2 poisoned the catalysts obviously. Supported Mn-Ce mixed-oxide catalysts, such as MnO_x-CeO_2/AC/C (Tang et al., 2007) and Mn-Ce/TiO_2 (Wu et al., 2008, 2009) have also exhibited high activity for low-temperature SCR of NO with NH_3. However, the activity of the catalysts decreased gradually along with the reaction in the presence of SO_2. Recently, Fe-based catalysts, such as Fe-TiO_2-PILC (Long and Yang, 1999), Fe_xTiO_y (Liu et al., 2008) and $Fe_xMn_{1-x}TiO_y$ (Liu et al., 2009) have been reported to be highly active and resistant to H_2O/SO_2 for SCR of NO with NH_3 in the medium temperature range. For Mn/TiO_2 catalysts, the addition of iron oxides was found to increase the NO conversion and resistance to H_2O/SO_2 for low temperature SCR of NO with NH_3 (Qi and Yang, 2003).

In our recent study, the catalyst of iron doped Mn-Ce/TiO_2 (Fe-Mn-Ce/TiO_2) seemed to be more active and more resistant to SO_2 than that of Mn-Ce/TiO_2. Therefore, Fe-Mn-Ce/TiO_2 was studied to remove NO with NH_3 at low temperature. The effects of H_2O and residue SO_2 in flue gases on the activity of the catalysts for low-temperature SCR of NO with NH_3 were also investigated.

* Corresponding author. E-mail: shenboxiong0722@sina.com

1 Materials and methods

1.1 Catalyst preparation

The preparation of Mn-Ce/TiO_2 was carried out by sol-gel method. All chemicals were obtained from Tianjin Guangfu Fine Chemical Research Institute (China). Butyl titanate was used as the precursor of titanium dioxide, manganese nitrate ($Mn(NO_3)_2$) and cerium nitrate ($Ce(NO_3)_3$) as the sources of manganese oxides and cerium oxides, respectively. A certain amount of butyl titanate (0.1 mol, analytical grade) and absolute alcohol (0.4 mol, analytical grade) were mixed under vigorous stirring at room temperature to obtain solution A, and acetic acid (0.3 mol, analytical grade) and absolute alcohol (0.4 mol, analytical grade) were dissolved in deionized water (0.4 mol) to obtain solution B. Subsequently, the solution B was dropped into the solution A under vigorous stirring to obtain transparent sol. A proper amount of $Mn(NO_3)_2$ and $Ce(NO_3)_3$ were added during this process. The molar ratios of Mn/Ti and Ce/Ti were 0.2:1 and 0.3:1, respectively. The transparent sol was kept at room temperature for several days, and then transformed to gel. Then the gel was dried at 80°C for 24 hr to remove organic solution and then calcined in muffle furnace at 500°C for 6 hr to obtain the catalysts of Mn-Ce/TiO_2. Following the same procedure, iron doped Mn-Ce/TiO_2 catalysts were prepared using ferric nitrate ($Fe(NO_3)_3$, analytical grade) as precursor. $Fe(NO_3)_3$ was added together with $Mn(NO_3)_2$ and $Ce(NO_3)_3$ during the catalyst preparation. The resulted catalysts were denoted as Fe(x)-Mn-Ce/TiO_2, where x represented the molar ratio of Fe/Ti, e.g., Fe(0.1)-Mn-Ce/TiO_2.

1.2 Catalytic activity test

The SCR activity of the catalysts for NO removal with NH_3 was carried out in a fixed-bed flow reactor. Six gas streams, 0.06 vol% NO, 0.06 vol% NH_3, 3 vol% O_2, 3 vol% H_2O (when used), 0.01 vol% SO_2 (when used) and pure N_2 in balance were used to simulate the flue gas. The catalytic activities for NO conversion to NO_2 were also measured. The reactant gas consisted of 0.06 vol% NO, 3 vol% O_2, and pure N_2 in balance. In all the runs, the total gas flow rate was maintained at 300 mL/min over 0.5 g catalyst (60–80 mesh) corresponding to a gas hourly space velocity (GHSV) of 50,000 hr^{-1}. The feed gases were mixed and preheated in a chamber before entering the reactor. The water vapor was generated by passing N_2 through a heated gas-wash bottle containing deionized water (80°C). During the measurements, the concentrations of NO and NO_2 at the inlet and outlet of the reactor were monitored by Flue Gas Analyzer (KM900/KM9106, Kane International Ltd., United Kingdom) equipped with NO, NO_2 and SO_2 sensor.

1.3 Catalyst characterization

A NOVA 2000 automated gas sorption system (Quantachrome Instruments, USA) was used to measure the physical properties of the catalysts at liquid N_2 temperature (–196°C). The specific surface area, pore volume and pore size distribution of the catalysts were determined by BET and BJH methods. The powder X-ray diffraction (XRD) measurement was used to analyze the crystal structure of the catalysts with Rigaku D/Max 2500 system using Cu K_α radiation (40 kV, 100 mA) (Rigaku Corporation, Japan). The surface atomic state of the catalysts was determined by X-ray photoelectron spectroscopy (XPS) using Kratos Axis Ultra DLD spectrometer equipped with a monochromated Al K_α radiation (1486.6 eV) (Shimadzu Corporation, Japan). The binding energy calibration was checked by the line position of C1s as an internal reference (284.6 eV). The normal operating pressure in the analysis chamber was controlled to 10^{-9} Pa during the measurement.

The temperature programmed desorption (NH_3-TPD and NOx-TPD) was performed on tp-5080 automated chemisorption analyzer using 0.1 g catalysts. The experiment started with a pretreatment in pure N_2 at 500°C for 1 hr. Subsequently, the catalyst was cooled down to room temperature in pure N_2 and then saturated for 30 min with a stream of pure NH_3 (or 20 vol% NO + 3 vol% O_2/N_2) (total flow rate = 1 mL/min (STP)). After saturation, the catalysts were flushed in a pure N_2 flow for 30 min at 100°C. Finally, the TPD of NH_3 (or NOx) was carried out in pure N_2 at a heating rate of 5°C/min from 5°C/min from 100 to 400°C. The NH_3 (or NOx) desorption were measured quantitatively by a thermal conductivity detector (TCD).

2 Results and discussion

2.1 TiO_2 supported different metallic oxides

2.1.1 Activity of TiO_2 supported metallic oxides

In order to compare the activities of TiO_2 supported various metallic oxides, different catalysts such as Fe(0.1)-Mn-Ce/TiO_2, Fe(0.1)-Mn/TiO_2, Fe(0.1)-Ce/TiO_2, and Fe(0.1)/TiO_2 were also prepared by sol-gel method as Mn-Ce/TiO_2. In all samples, the ratios of Mn/Ti and Ce/Ti were 0.2:1 and 0.3:1, respectively. Figure 1 shows the NO conversion for the SCR of NO with NH_3 over the catalysts of TiO_2 supported various metallic oxides at 80–260°C. It can be seen from Fig. 1 that the NO conversion over all the catalysts increased with increasing temperature. Among the catalysts, Fe(0.1)/TiO_2 showed the lowest activity and only 30% NO conversion was obtained when the temperature reached 260°C. For TiO_2 supported Mn-Ce, Fe-Mn and Fe-Ce catalysts, Mn-Ce/TiO_2 exhibited higher NO conversion than that over Fe(0.1)-Mn/TiO_2 and Fe(0.1)-Ce/TiO_2 catalysts. It should be noted that the catalytic activity of Mn-Ce/TiO_2 was improved greatly after the iron doping, and the highest NO conversion was obtained over Fe(0.1)-Mn-Ce/TiO_2 especially within the low temperature range of 80–200°C. NO conversion (96.8%) was obtained over this catalyst at 180°C at a space velocity of 50,000 hr^{-1}. Based on the results from Fig. 1, it could be concluded that iron doping was favorable to improve the activity of Mn-Ce/TiO_2 for low-temperature

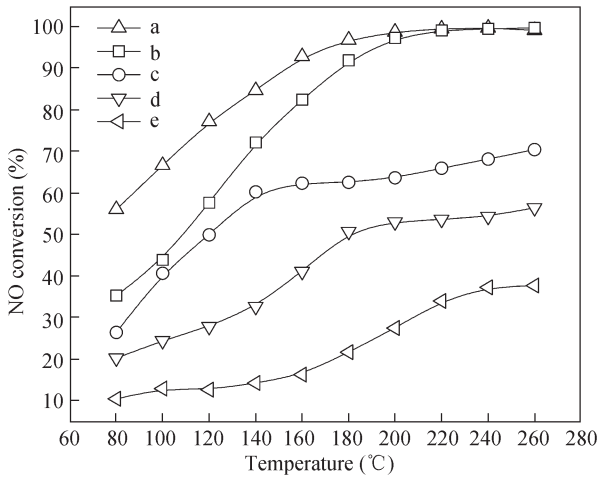

Fig. 1 NO conversion over TiO_2 supported metallic oxides at different temperatures. (a) Fe(0.1)-Mn-Ce/TiO_2; (b) Mn-Ce/TiO_2; (c) Fe(0.1)-Mn/TiO_2; (d) Fe(0.1)-Ce/TiO_2; (e) Fe(0.1)/TiO_2. Reaction conditions: 0.06 vol% NO, 0.06 vol% NH_3, 3 vol% O_2, balance N_2, GHSV 50,000 hr^{-1}, total flow rate 300 mL/min.

SCR of NO with NH_3.

2.1.2 XRD analysis of TiO_2 supported metallic oxides

Figure 2 shows XRD patterns of TiO_2 supported metallic oxides. For Fe(0.1)-Mn/TiO_2 and Fe(0.1)-Ce/TiO_2, the reflections provided typical diffraction peaks as attributive indicator of TiO_2 anatase phase (2θ = 25.2°, 38.0°, 48.1°, 54.5°, 62.8°, 70.3°, 75.3°) and TiO_2 rutile phase (2θ = 27.4°, 36.0°, 41.2°). It meant that TiO_2 in the catalysts existed in the form of anatase and rutile, and anatase was the dominating structure. For Mn-Ce/TiO_2, only strong peaks as indicator of TiO_2 anatase phase were observed in the XRD pattern. It was known that TiO_2 anatase phase as the support of SCR catalyst was more active than TiO_2 rutile phase (Forzatti, 2000; Jiang et al., 2009). In above TiO_2 supported Mn-Ce, Fe-Mn and Fe-Ce catalysts, none of XRD patterns gave intense peaks for crystalline promoters (Mn-Ce, Fe-Mn and Fe-Ce), which indicated the high dispersion or poorly crystalline state of promoter atoms. For Fe(0.1)-Mn-Ce/TiO_2, the intensity of all of peaks corresponded to TiO_2 anatase phase decreased compared with that on Mn-Ce/TiO_2 XRD curve, indicating that iron doping inhibited the appearance of TiO_2 anatase phase in the XRD pattern. And no intense peaks for Mn, Ce and Fe were observed in the XRD pattern of Fe(0.1)-Mn-Ce/TiO_2.

2.2 Fe-Mn-Ce/TiO_2 catalysts

2.2.1 Activity of Fe-Mn-Ce/TiO_2 catalysts

According to the results from Fig. 1, iron doping had positive effect on the activity of the catalysts. In this work, it was interesting to clarify the effects of iron loadings on the activity of Fe-Mn-Ce/TiO_2 for low-temperature SCR of NO with NH_3. In Fig. 3, it could be seen that increasing the molar ratio of Fe/Ti from 0 to 0.1 enhanced the NO conversion in the temperature range of 80–260°C. For Fe(0.1)-Mn-Ce/TiO_2, 56.1% NO conversion was obtained at 80°C and nearly 100% NO conversion in a wide temperature range (200–260°C). Further increase of the molar ratio of Fe/Ti from 0.1 to 0.2 lowered the activity of the catalysts. Figure 3 shows that the SCR activity increased following the sequence: Mn-Ce/TiO_2 < Fe(0.05)-Mn-Ce/TiO_2 < Fe(0.2)-Mn-Ce/TiO_2 < Fe(0.15)-Mn-Ce/TiO_2 < Fe(0.1)-Mn-Ce/ TiO_2.

2.2.2 XRD analysis of Fe-Mn-Ce/TiO_2 catalysts

The XRD patterns of Fe-Mn-Ce/TiO_2 with different iron loadings are shown in Fig. 4. At low loadings (the molar ratio of Fe/Ti < 0.15), the XRD patterns showed the presence of TiO_2 anatase phase, while no visible phases of Fe, Mn and Ce were observed in the XRD patterns. The intensities of peaks due to TiO_2 anatase phase decreased with the increasing of the molar ratio of Fe/Ti. As the molar ratio of Fe/Ti further increased from 0.15 to 0.2, all XRD peaks for TiO_2 anatase phase disappeared. It indicated that TiO_2 as support was covered with iron which inhibited the appearance of TiO_2 anatase phase in the XRD patterns. Peña et al. (2004) has also reported the observations that no XRD phases were observed for Fe/TiO_2, which was due to the high iron loading on the surface of TiO_2.

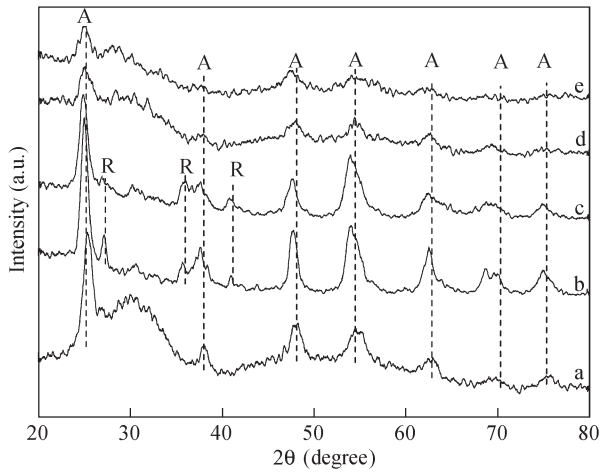

Fig. 2 XRD patterns of TiO_2 supported metallic oxides. Line a: Mn-Ce/TiO_2; line b: Fe(0.1)-Mn/TiO_2; line c: Fe(0.1)-Ce/TiO_2; line d: Fe(0.1)-Mn-Ce/TiO_2; line e: Fe/TiO_2. A: anatase; R: rutile.

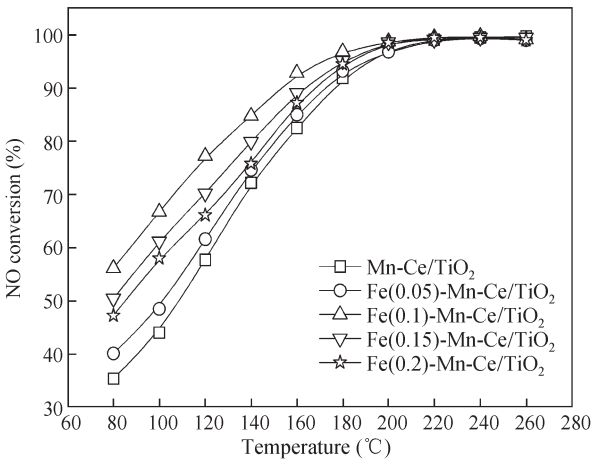

Fig. 3 NO conversion over Fe-Mn-Ce/TiO_2 catalysts with different Fe loadings. Reaction conditions: 0.06 vol% NO, 0.06 vol% NH_3, 3 vol% O_2, balance N_2, GHSV 50,000 hr^{-1}, total flow rate 300 mL/min.

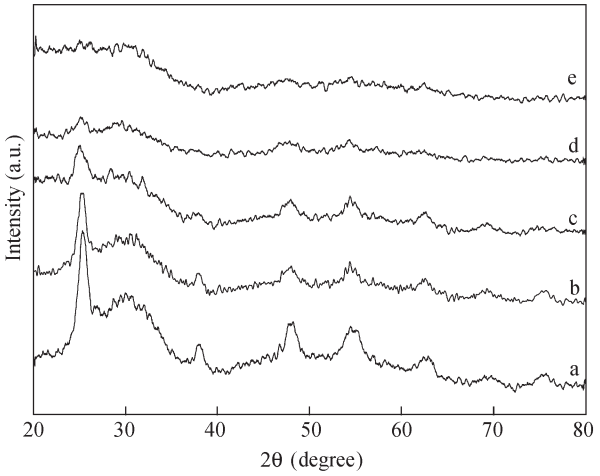

Fig. 4 XRD patterns of Fe-Mn-Ce/TiO_2 catalysts with different Fe loadings. Line a: Mn-Ce/TiO_2; line b: Fe(0.05)-Mn-Ce/TiO_2; line c: Fe(0.1)-Mn-Ce/TiO_2; line d: Fe(0.15)-Mn-Ce/TiO_2; line e: Fe(0.2)-Mn-Ce/TiO_2.

2.2.3 N_2 adsorption and TPD analysis for Fe-Mn-Ce/TiO_2 catalysts

Brunauer-Emmett-Teller (BET) specific surface area, pore volume and pore diameter of the catalysts with different iron loadings are summarized in Table 1. For Mn-Ce/TiO_2, the specific surface area was determined to be 87.46 m^2/g, and pore volume was 0.23 mL/g. After doping with iron, the specific surface area and pore volume of the catalysts increased while pore diameter decreased slightly. Therefore, the effect of iron doping could help to increase the specific surface area of the catalysts compared with that of Mn-Ce/TiO_2. However, as the molar ratio of Fe/Ti increased from 0.1 to 0.2, the specific surface area of iron doped catalysts did not increase further with the addition of iron. From Fig. 3 and Table 1, it could be seen that the variation in specific surface area of iron doped catalysts was in good agreement with the catalytic activity. Fe(0.1)-Mn-Ce/TiO_2 with the largest specific surface area in all the samples showed the best SCR activity.

Temperature programmed desorption experiments of NH_3 and NO*x* have been carried out to investigate the adsorption of NH_3 and NO*x* on the catalysts. Figure 5a shows the results of the NH_3-TPD runs performed over Mn-Ce/TiO_2 and Fe-Mn-Ce/TiO_2 catalysts. In all the cases the spectra showed similar features, with a broad shape in a wide temperature range (100–400°C). This clearly indicated the presence of several NH_3 adsorbed species with different thermal stability on the surface of the catalysts. After iron doping, NH_3 adsorption capacity of the catalysts

Table 1 Physical properties of the catalysts with different Fe loadings

Sample	Specific surface area (m^2/g)	Pore volume (mL/g)	Pore diameter (nm)
Fe(0)-Mn-Ce/TiO_2	87.46	0.2294	10.49
Fe(0.05)-Mn-Ce/TiO_2	95.28	0.2612	10.96
Fe(0.1)-Mn-Ce/TiO_2	121.6	0.2726	8.969
Fe(0.15)-Mn-Ce/TiO_2	116.8	0.2730	9.631
Fe(0.2)-Mn-Ce/TiO_2	103.4	0.2949	10.10

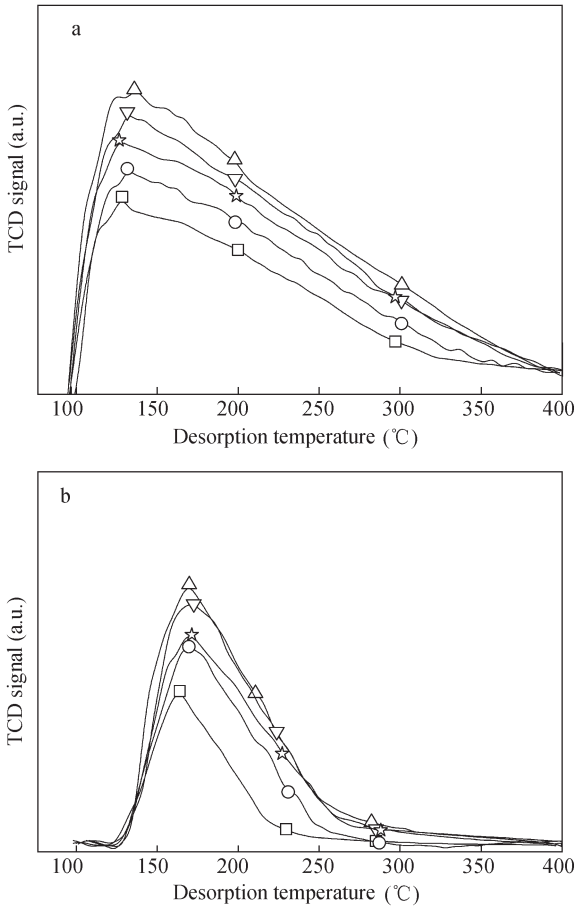

Fig. 5 TPD spectra of NH_3 (a) and NO*x* (b) over the catalysts.

increased greatly compared with that of Mn-Ce/TiO_2. The improvement in NH_3 adsorption capacity is believed to be beneficial to SCR reaction (Choi et al., 1996). NO*x*-TPD results over Mn-Ce/TiO_2 and Fe-Mn-Ce/TiO_2 catalysts are shown in Fig. 5b. All the catalysts exhibited one obvious NO*x* desorption peak centered at about 170°C. Similar with NH_3-TPD results, NO*x* adsorption capacity of Fe-Mn-Ce/TiO_2 catalysts also increased compared with Mn-Ce/TiO_2. Moreover, the NH_3 and NO*x* adsorption capacity of Fe-Mn-Ce/TiO_2 catalysts with different iron loadings changed in the same trend with its specific surface area as shown in Table 1. Therefore, it is feasible to believe that iron doped catalysts with large specific surface area and high NH_3 and NO*x* adsorption capacity exhibited high activity for low temperature SCR of NO with NH_3.

2.2.4 XPS analysis of Fe-Mn-Ce/TiO_2 catalysts

Table 2 shows the atomic concentrations on the surface of the catalysts determined by XPS. From Table 2, the concentrations of Mn, Ce and Ti on the surface of the catalysts decreased while the concentration of Fe increased with the addition of iron. In all samples, the molar ratios of Mn/Ti and Ce/Ti in the bulk were 0.2 and 0.3, respectively, while the ratios of Mn/Ti and Ce/Ti on the surface of the catalysts increased greatly according to the XPS results, which indicated that Mn and Ce were easy to disperse on the surface of the catalysts. Fe also had high dispersion on the surface of iron doped catalysts. The ratio of Fe/Ti

Table 2 Atomic concentrations (%) on the surface of the catalysts determined by XPS

Samples	Ti	Mn	Mn/Ti	Ce	Ce/Ti	Fe	Fe/Ti	O_t		
								O_t	O_α	O_β
Mn-Ce/TiO_2	18.64	5.67	0.30	8.0	0.43	0.00	0.00	67.66	25.03	42.63
Fe(0.1)-Mn-Ce/TiO_2	15.56	5.29	0.34	7.16	0.46	3.53	0.23	68.46	33.78	34.68
Fe(0.2)-Mn-Ce/TiO_2	13.12	4.33	0.33	6.13	0.47	6.24	0.48	70.18	32.98	37.2

O_t is oxygen concentration, which is composed of lattice oxygen (denoted as O_β) and chemisorbed oxygen (denoted as O_α).

on the surface of Fe(0.1)-Mn-Ce/TiO_2 was 0.23, which was twice as much as that in the bulk. For Fe(0.2)-Mn-Ce/TiO_2, the surface Fe/Ti ratio reached 0.48 which was much higher than that in the bulk (Fe/Ti = 0.2). Due to the high surface Fe/Ti ratio, Fe would deposit on the surface of TiO_2, which might lead to the disappearance of TiO_2 anatase phase in the XRD patterns as shown in Fig. 4. It is also interesting to find that the ratios of Mn/Ti and Ce/Ti on the surface of iron doped catalysts increased compared with that of Mn-Ce/TiO_2. Therefore, it could be concluded that iron doped catalysts enhanced the dispersion of Mn and Ce on the surface of the catalysts. The oxygen concentrations (denoted as O_t) on the surface of the catalysts were found to increase after the doping of iron. O_t was composed of lattice oxygen (denoted as O_β) and chemisorbed oxygen (denoted as O_α). Lattice oxygen on the surface of Fe-Mn-Ce/TiO_2 catalysts was found to decrease while chemisorbed oxygen was found to increase compared with that of Mn-Ce/TiO_2.

Figure 6a shows the Mn2p spectra of the catalysts investigated. For the catalysts of Fe-Mn-Ce/TiO_2 and Mn-Ce/TiO_2, two peaks at 641.7 and 653.3 eV corresponded to $Mn2p_{3/2}$-$Mn2p_{1/2}$ doublet, which had been reported to be characteristic of a mixed-valence manganese system (Mn^{3+} and Mn^{4+}) (Wu et al., 2008; Zhang et al., 2007). Additionally, a shake-up satellite with the binding energy of about 646 eV was also observed in the Mn2p spectra. Previous reports had also found the formation of the shake-up satellite, which could be attributed to the presence of Mn^{2+} species on the surface of the catalysts (Castro et al., 1989; Beyreuther et al., 2006). For iron doped catalysts, there was no energetic shift of the Mn2p spectra after the iron doping, but the concentration of Mn^{2+} decreased compared with that of Mn-Ce/TiO_2. The ratio of (Mn^{3+}+

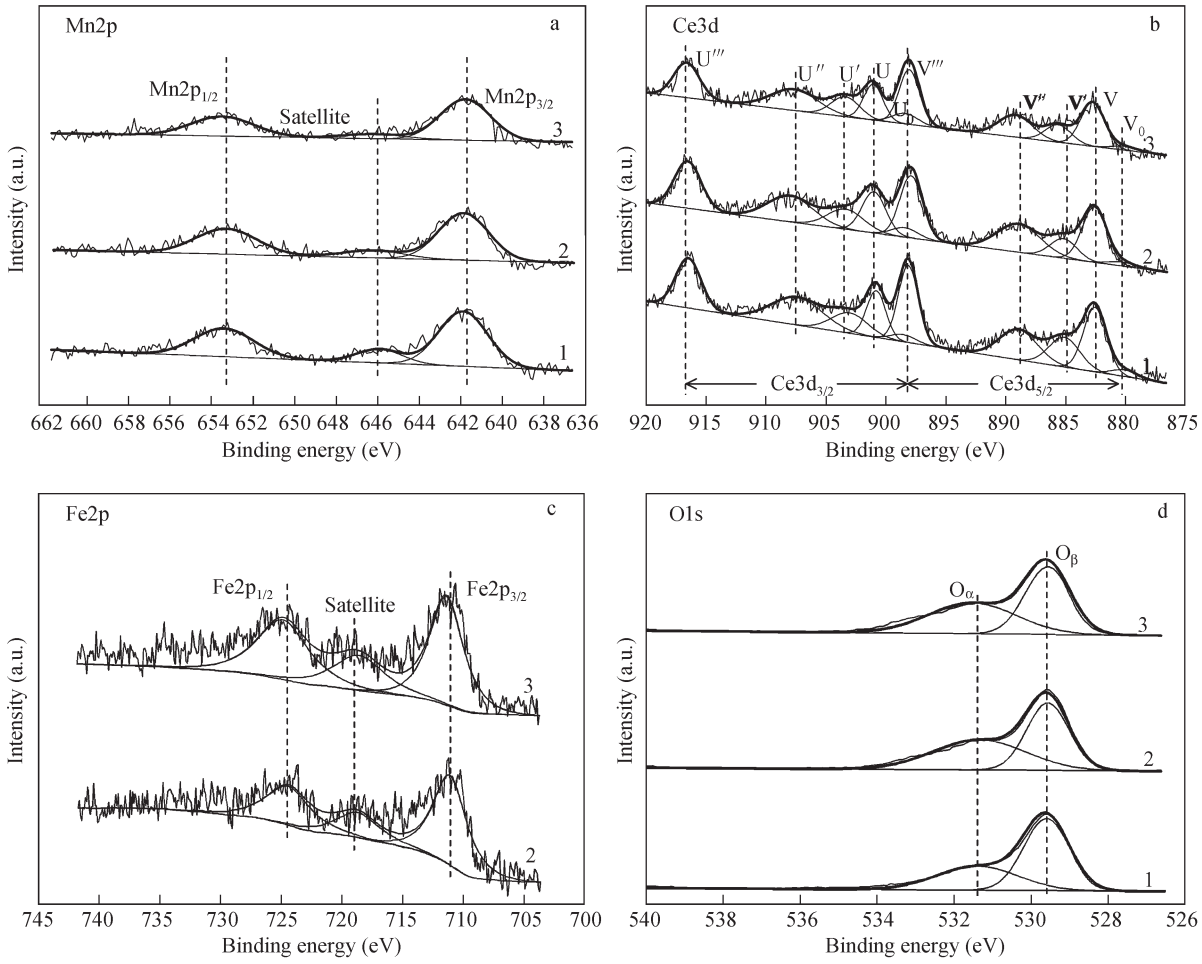

Fig. 6 Mn2p (a), Ce3d (b), Fe2p (c), and O1s (d) XPS spectra of the catalysts. Line 1: Mn-Ce/TiO_2; line 2: Fe(0.1)-Mn-Ce/TiO_2; line 3: Fe(0.2)-Mn-Ce/TiO_2.

Mn^{4+})/Mn^{2+} was 6.89 for Mn-Ce/TiO_2, and it increased to 8.54 and 11.67 for Fe(0.1)-Mn-Ce/TiO_2 and Fe(0.2)-Mn-Ce/TiO_2, respectively. Therefore, it could be seen that iron doped catalysts enhanced the oxidation state of Mn on the surface of the catalysts.

The typical examples of observed Ce3d spectra are presented in Fig. 6b. According to previous reports (Patsalas and Logothetidis, 2003; Chang et al., 2006), XPS peaks denoted as V (882.5 eV), V″ (888.8 eV), and V‴ (898.4 eV) and U (901.0 eV), U″ (907.5 eV), and U‴ (916.7 eV) were assigned to Ce^{4+} species while U_0 (898.8 eV), U′ (903.5 eV), V_0 (880.3 eV), and V′ (884.9 eV) were attributed to Ce^{3+} species. According to this theory, tetravalent Ce^{4+} and trivalent Ce^{3+} were considered to coexist on the surface of the catalysts in our studies. The ratio of Ce^{4+}/Ce^{3+} was calculated from the XPS spectra, inspired by an XPS investigation of Chang et al. (2006). The results showed that the ratio of Ce^{4+}/Ce^{3+} was about 3.78, 4.60 and 3.97 for Mn-Ce/TiO_2, Fe(0.1)-Mn-Ce/TiO_2, and Fe(0.2)-Mn-Ce/TiO_2, respectively. From the results, we could learn that Ce^{4+} oxidation state was predominant, and Ce^{3+} was weak compared with Ce^{4+}. It should be noted that the ratio of Ce^{4+}/Ce^{3+} increased after the doping of iron. Therefore, iron doped catalysts of Fe-Mn-Ce/TiO_2 had higher oxidation state of Ce than that of Mn-Ce/TiO_2. Moreover, Fe(0.1)-Mn-Ce/TiO_2 with the highest ratio of Ce^{4+}/Ce^{3+} showed the best SCR activity, which indicated that there might be some relations between the activity and the ratio of Ce^{4+}/Ce^{3+} on the surface of the catalysts.

Fe2p spectra from the catalysts investigated contained $Fe2p_{3/2}$ and $Fe2p_{1/2}$ doublet with maximum intensities at 711.1 and 724.5 eV (Fig. 6c). It has been reported that Fe_2O_3 oxides are characterized by $Fe2p_{3/2}$ binding energies in the range of 711.0–711.2 eV (Roosendaal et al., 1999; Doscostes et al., 2000). And the formation of weak shake-up satellite offset from the basic photoelectron lines of $Fe2p_{3/2}$ by 8 eV towards higher binding energies indicated the predominant formation of Fe^{3+} ions (Bukhtiyarova et al., 2009). These data would help us to identify the spectra from our samples. The weak shake-up satellite peak at about 719 eV observed in the Fe2p spectra for iron doped catalysts indicated that all iron ions on the surface of the catalysts were exclusively in Fe^{3+} state.

The XPS spectra for O1s (Fig. 6d) showed that the O1s spectra gave two distinct peaks. The peak at 529.6–530.0 eV corresponded to lattice oxygen (denoted as O_β) while the one at 531.3–531.7 eV corresponded to chemisorbed oxygen (denoted as O_α) (Kang et al., 2007). The concentration of O_β from metal oxides decreased after the doping of iron. The ratio of total metal (Fe, Mn, Ce and Ti) to O_β was 0.76 for Mn-Ce/TiO_2, and it increased to 0.91 and 0.81 for Fe(0.1)-Mn-Ce/TiO_2 and Fe(0.2)-Mn-Ce/TiO_2, respectively. The reason for this change might be due to the dispersion of iron on the surface of the catalysts while Fe^{3+} needing less lattice oxygen compared with that of Mn^{4+} and Ce^{4+}. The surface chemisorbed oxygen has been reported to be helpful in the oxidation of NO to NO_2 (Wu et al., 2008), which are favorable to the reduction of NO in the SCR process. From Fig. 6d and Table 2, O_α concentration on the surface of the catalysts increased greatly after the doping of iron. Figure 7 shows the activity of Mn-Ce/TiO_2 and Fe-Mn-Ce/TiO_2 catalysts for the oxidation of NO to NO_2 at 80–260°C. The NO conversion to NO_2 over Fe(0.1)-Mn-Ce/TiO_2 and Fe(0.2)-Mn-Ce/TiO_2 showed an obvious enhancement compared with Mn-Ce/TiO_2. Fe(0.1)-Mn-Ce/TiO_2 with the highest O_α concentration on the surface of the catalysts showed the best SCR activity at low temperature. Therefore, increasing chemisorbed oxygen concentration on the surface of the catalysts might have positive effect on the SCR reaction, which was consistent with the results from the SCR activity tests.

2.2.5 Activity of Fe-Mn-Ce/TiO_2 in the presence of H_2O and SO_2

Because the low temperature SCR catalyst is usually deactivated mainly by water vapor (H_2O) and residue SO_2 in the flue gases, it is necessary to investigate the resistance of the catalysts to H_2O and SO_2 at low temperature. Figure 8 compares the NO conversion over Fe-Mn-Ce/TiO_2 and

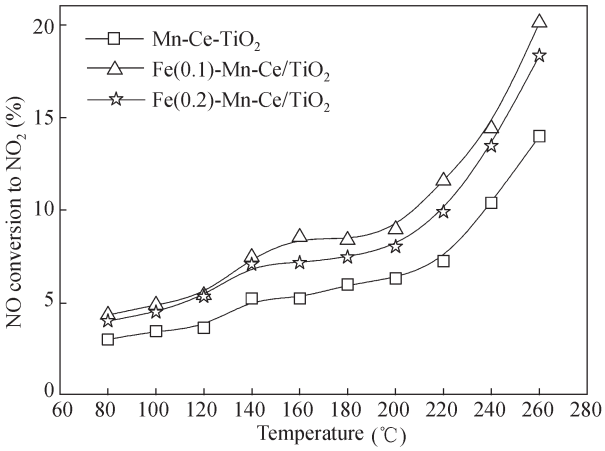

Fig. 7 Oxidation of NO to NO_2 over Mn-Ce/TiO_2 and Fe-Mn-Ce/TiO_2 catalysts. Reaction conditions: 0.06 vol% NO, 3 vol% O_2, balance N_2, GHSV 50,000 hr^{-1}, total flow rate 300 mL/min.

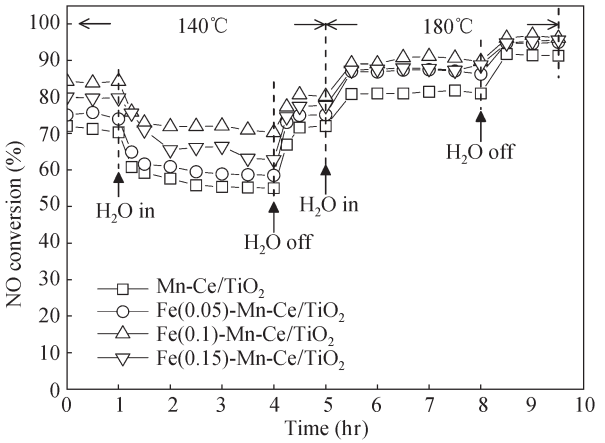

Fig. 8 Effect of H_2O on NO conversion over Mn-Ce/TiO_2 and Fe-Mn-Ce/TiO_2 catalysts. Reaction conditions: 0.06 vol% NO, 0.06 vol% NH_3, 3 vol% O_2, 3 vol% H_2O (when used), balance N_2, GHSV 50,000 hr^{-1}, total flow rate 300 mL/min.

Mn-Ce/TiO_2 at 140 and 180°C in the presence of 3 vol% H_2O. Before the addition of H_2O, the SCR reaction has been stabilized for 1 hr at 140°C. When 3 vol% H_2O was added into the flue gases, the NO conversion at 140°C over Fe(0.1)-Mn-Ce/TiO_2 decreased from 81.2% to 70%. After 3 hr SCR reaction in the presence of 3 vol% H_2O, H_2O was removed from the flue gases and the NO conversion almost recovered. After another 1 hr of steady reaction at 140°C (the NO conversion almost stabilized at 81%), the SCR temperature increased to 180°C and 3 vol% H_2O was fed once again. It was found that the NO conversion almost kept a steady level of 90% within 3 hr. When the supply of H_2O was ended, the NO conversion restored to 96%, almost near 96.5% conversion at 180°C in the absence of H_2O. Similar effects of H_2O on the NO conversion were observed over Mn-Ce/TiO_2 catalysts. The results clearly indicated that H_2O exhibited a reversible, inhibiting effect on the activity of the catalysts at different temperatures. The reasons should be that the presence of gas phase water in the flue gases inhibited the reactant adsorption over the catalyst surface and the reduced adsorption of reactant caused the reversible effect on the activity of the catalysts. From Fig. 8, it can also be seen that H_2O exhibited much more severe effect on NO conversion of Mn-Ce/TiO_2 than that of Fe-Mn-Ce/TiO_2. NO conversion over Mn-Ce/TiO_2 decreased from 70% to 56% at 140°C in the presence of H_2O and increased from 81% to 92% at 180°C after cutting off of the H_2O supply. The SCR activity in the presence of H_2O increased following the sequence: Mn-Ce/TiO_2 < Fe(0.05)-Mn-Ce/TiO_2 < Fe(0.15)-Mn-Ce/TiO_2 < Fe(0.1)-Mn-Ce/TiO_2.

The synergistic effect of H_2O and SO_2 on the NO conversion over Fe-Mn-Ce/TiO_2 catalysts is shown in Fig. 9 and compared with that over Mn-Ce/TiO_2 at 180°C. As shown in Fig. 9, when 3 vol% H_2O and 0.01 vol% SO_2 were added into the flue gases, the NO conversion over Mn-Ce/TiO_2 decreased from the initial 91.8% to 49.5% in 5 hr. The deactivation of Mn-Ce/TiO_2 by H_2O and SO_2 at low temperature was consistent with the observations over other SCR catalysts in previous literatures (Wu et al., 2009; Casapu et al., 2009). At low temperature, SO_2 could be adsorbed by metal oxides in the catalysts and produced metal sulphates. On the other hand, some ammonium sulfates (such as NH_4HSO_4 and $(NH_4)_2SO_4$) would be formed by the reaction between SO_2 and the reactants (NH_3 and O_2). The formed metal sulphates and ammonium sulfates would occupy active sites on the surface of catalysts and gradually deactivated the catalysts along with the reaction. Compared with the deactivation of Mn-Ce/TiO_2 by H_2O and SO_2, the deactivation of the catalysts was reduced after the doping of iron. Moreover, it was found that the resistance of iron doped catalysts to H_2O and SO_2 was enhanced with the increasing of iron loadings. Fe(0.15)-Mn-Ce/TiO_2 showed higher resistance to H_2O and SO_2 than 0.05 and 0.1 of iron doped catalysts, and still provided 83.8% NO conversion in further 5 hr. The promotion effect on resistance to H_2O and SO_2 has also been reported for MnO_x-CeO_2 (Qi et al., 2004) catalysts. It was indicated that the addition of iron oxide significantly decreased the rate of formation of sulfate, thus inhibited deactivation (Qi and Yang, 2003). It could also be seen from Fig. 9 that the NO conversion over all samples recovered slightly after H_2O and SO_2 were turned off. This might be due to the recovery from the reversible inhibition by water vapor as shown in Fig. 8.

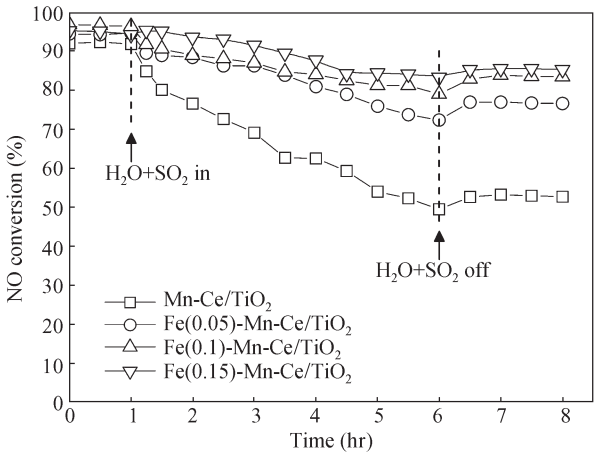

Fig. 9 Effect of H_2O and SO_2 on NO conversion over Mn-Ce/TiO_2 and Fe-Mn-Ce/TiO_2 catalysts. Reaction conditions: 0.06 vol% NO, 0.06 vol% NH_3, 3 vol% O_2, 3 vol% H_2O (when used), 0.01 vol% SO_2 (when used), balance N_2, GHSV 50,000 hr^{-1}, total flow rate 300 mL/min.

3 Conclusions

Iron doped catalysts of Fe-Mn-Ce/TiO_2 exhibited high activity for low temperature SCR of NO with NH_3 at 80–260°C. The iron doping enhanced the resistance of Fe-Mn-Ce/TiO_2 to H_2O and SO_2 greatly. Among the iron doped catalysts, Fe(0.1)-Mn-Ce/TiO_2 showed the highest SCR activity in the absence of H_2O and SO_2, and Fe(0.15)-Mn-Ce/TiO_2 exhibited the best resistance to H_2O and SO_2. The inhibiting effect of H_2O on the activity of the catalysts at 140 and 180°C was reversible, but the deactivation by SO_2 hardly recovered.

BET and NH_3-TPD results showed that iron doping could help to increase the specific surface area and NH_3 adsorption capacity of the catalysts. It was known from XPS analysis that iron valence state on the surface of the catalysts were in Fe^{3+} state. Iron doping enhanced the dispersion and oxidation state of Mn and Ce on the surface of the catalysts. The oxygen concentrations on the surface of the catalysts were found to increase after the doping of iron. Lattice oxygen on the surface of Fe-Mn-Ce/TiO_2 catalysts was found to decrease while chemisorbed oxygen was found to increase compared with that of Mn-Ce/TiO_2.

Acknowledgments

This work was supported by the National Natural Science Foundation of China (No. 90610018, 50976050), the New Century Excellent Talents in University (No. NCET-07-0457) and the National Key Technologies R&D Program of Tianjin (No. 09ZCKFSH01900).

References

Beyreuther E, Grafström S, Eng L M, 2006. XPS investigation of Mn valence in lanthanum manganite thin films under variation of oxygen content. *Physical Review B*, 73 (15): 155425.

Bukhtiyarova M V, Ivanova A S, Plyasova L M, Litvak G S, Rogov V A, Kaichev V V et al., 2009. Selective catalytic reduction of nitrogen oxide by ammonia on Mn(Fe)-substituted Sr(La) aluminates. *Applied Catalysis A: General*, 357(2): 193–205.

Castro V D, Polzonetti G, 1989. XPS study of MnO oxidation. *Journal of Electron Spectroscopy and Related Phenomena*, 48(1): 117–123.

Choi E Y, Nam I S, Kim Y G, 1996. TPD study of mordenite-type zeolites for selective catalytic reduction of NO by NH_3. *Journal of Catalysis*, 161(2): 597–604.

Chang L H, Sasirekha N, Chen Y W, Wang W J, 2006. Preferential oxidation of CO in H_2 stream over Au/MnO_2-CeO_2 catalysts. *Industrial & Engineering Chemistry Research*, 45 (14): 4927–4935.

Casapu M, Kröcher O, Elsener M, 2009. Screening of doped MnO_x-CeO_2 catalysts for low-temperature NO-SCR. *Applied Catalysis B: Environmental*, 88(3-4): 413–419.

Doscostes M, Mercier F, Thromat N, Beaucaire C, Gautier-Soyer M, 2000. Use of XPS in the determination of chemical environment and oxidation state of iron and sulfur samples: constitution of a data basis in binding energies for Fe and S reference compounds and applications to the evidence of surface species of an oxidized pyrite in a carbonate medium. *Applied Surface Science*, 165(4): 288–302.

Forzatti P, 2000. Environmental catalysis for stationary applications. *Catalysis Today*, 62(1): 51–65.

Jiang B Q, Liu Y, Wu Z B, 2009. Low temperature selective catalytic reduction of NO on MnO_x/TiO_2 prepared by different methods. *Journal of Hazardous Materials*, 162(2-3): 1249–1254.

Kang M, Park E D, Kim J M, Yie J E, 2007. Manganese oxide catalysts for NO*x* reduction with NH_3 at low temperatures. *Applied Catalysis A: General*, 327(2): 261–269.

Long R Q, Yang R T, 1999. Selective catalytic reduction of nitrogen oxides by ammonia over Fe^{3+}-exchanged TiO_2-pillared clay catalysts. *Journal of Catalysis*, 186(2): 254–268.

Liu F D, He H, Zhang C B, 2008. Novel iron titanate catalyst for the selective catalytic reduction of NO with NH_3 in the medium temperature range. *Chemical Communications*, (17): 2043–2045.

Liu F D, He H, Ding Y, Zhang C B, 2009. Effect of manganese substitution on the structure and activity of iron titanate catalyst for the selective catalytic reduction of NO with NH_3. *Applied Catalysis B: Environmental*, 93(1-2): 194–204.

Park T S, Jeong S K, Hong S H, Hong S C, 2001. Selective catalytic reduction of nitrogen oxides with NH_3 over natural manganese ore at low temperature. *Industrial & Engineering Chemistry Research*, 40(21): 4491–4495.

Patsalas P, Logothetidis S, 2003. Structure-dependent electronic properties of nanocrystalline cerium oxide films. *Physical Review B*, 68(3): 035104.

Peña D A, Uphade B S, Smirniotis P G, 2004. TiO_2-supported metal oxide catalysts for low-temperature selective catalytic reduction of NO with NH_3: I. Evaluation and characterization of first row transition metals. *Journal of Catalysis*, 221(2): 421–431.

Qi G S, Yang R T, 2003. Low-temperature selective catalytic reduction of NO with NH_3 over iron and manganese oxides supported on titania. *Applied Catalysis B: Environmental*, 44(3): 217–225.

Qi G S, Yang R T, Chang R, 2004. MnO_x-CeO_2 mixed oxides prepared by co-precipitation for selective catalytic reduction of NO with NH_3 at low temperatures. *Applied Catalysis B: Environmental*, 51(2): 93–106.

Roosendaal S J, van Asselen B, Elsenaar J W, Vredenberg A M, 1999. The oxidation state of Fe(100) after initial oxidation in O_2. *Surface Science*, 442(3): 329–337.

Tang X L, Hao J M, Yi H H, Li J H, 2007. Low-temperature SCR of NO with NH_3 over AC/C supported manganese-based monolithic catalysts. *Catalysis Today*, 126(3-4): 406–411.

Wu Z B, Jin R B, Liu Y, Wang H Q, 2008. Ceria modified MnO_x/TiO_2 as a superior catalyst for NO reduction with NH_3 at low-temperature. *Catalysis Communications*, 9(13): 2217–2220.

Wu Z B, Jin R B, Wang H Q, Liu Y, 2009. Effect of ceria doping on SO_2 resistance of Mn/TiO_2 for selective catalytic reduction of NO with NH_3 at low temperature. *Catalysis Communications*, 10(6): 935–939.

Xu W Q, Yu Y B, Zhang C B, He H, 2008. Selective catalytic reduction of NO with NH_3 over a Ce/TiO_2 catalyst. *Catalysis Communications*, 9(6): 1453–1457.

Zhang X, Ji L Y, Zhang S C, Yang W S, 2007. Synthesis of a novel polyaniline-intercalated layered manganese oxide nanocomposite as electrode material for electrochemical capacitor. *Power Sources*, 173(2): 1017–1023.